

Origin of the tunneling states in SiO₂

C. Laermans and V. Keppens

Department of Physics, Katholieke Universiteit Leuven, Celestijnenlaan 200D, B-3001 Leuven, Belgium

(Received 17 October 1994)

Ultrasonic velocity change and attenuation measurements are performed in neutron-irradiated *z*-cut quartz, for three different doses. From numerical fits of the data using the tunneling model, the typical parameters of the tunneling states (TS) are determined and compared with those found in comparable *x*-cut samples (irradiated under the same conditions and with similar doses). This study reveals a remarkable anisotropy, which has to be attributed to the tunneling mechanism itself. In search of the microscopic origin of the tunneling states, these results give direct experimental evidence for a microscopic picture of the TS as a rotation of coupled SiO₄ tetrahedra. At the same time, they provide important evidence for the missing link to obtain a common interpretation of all three low-frequency excitations in vitreous silica.

I. INTRODUCTION

For about two decades, the low-temperature properties of amorphous materials have been successfully described by the tunneling model (TM),¹ assuming the existence of low-energy excitations, the so-called tunneling states (TS). In spite of its success, this model is purely phenomenological and the microscopic origin of the TS remains unknown. In the search for an identification of this microscopic nature, defective crystals turned out to be very interesting. In our laboratory, a systematic study of the TS in neutron- and electron-irradiated *x*-cut quartz is being carried out by means of ultrasonic measurements.^{2,3} From this study, it became clear that the tunneling states cannot only be contained in amorphous regions; a considerable part of the TS has to be attributed to the remaining distorted "crystalline" fraction of the samples. In view of the microscopic origin of the TS, an important question arises now: what is the damage in the crystalline part of the sample which can account for the observed TS? This paper will address this question: ultrasonic measurements are carried out in neutron-irradiated *z*-cut quartz and provide experimental evidence for a microscopic description of at least part of the TS in neutron-irradiated quartz.

The key idea to approach *z*-cut samples is the following: the damaged "crystalline" part of neutron-irradiated quartz is known to contain radiation-induced Dauphiné twins: groups of SiO₄ tetrahedra which are rotated 180° with respect to each other.⁴ The idea rose that the "crystalline" TS could be related to these twins, but up to now experiments which could give evidence in favor of or against such a description of the TS were still lacking. A comparison of the TS in previously studied neutron-irradiated *x*-cut quartz with the TS in similar *z*-cut specimens might, however, reveal important information on this issue: since the movements involved in the twinning motion take place mainly in the *xy* plane, a longitudinal wave traveling in this plane is expected to induce more easily a transition of a tetrahedron (or chains of tetrahedra) than a wave in any other direction. If the TS are re-

lated to the twins, this would lead to an anisotropic coupling of the TS with the longitudinal phonons. Therefore we performed ultrasonic measurements as a function of temperature in *z*-cut quartz samples, irradiated under the same conditions and with similar doses as the *x*-cut samples studied before. But, whereas the applied longitudinal wave propagated along the crystallographic *x* axis in the *x*-cut samples, the *z*-cut samples are probed along the *z* axis. This allows one to investigate the possible influence of the direction of the wave propagation on the coupling with the TS. Three different doses are studied, and both attenuation and velocity measurements have been carried out. This gives an extensive set of data, allowing a profound and reliable analysis. Numerical fits of the data, using the tunneling model, are carried out; the typical TS parameters are determined and compared with those found in comparable *x*-cut samples. Remarkable anisotropic behavior is seen, leading to important evidence for a microscopic description of the tunneling states in SiO₂.

II. THEORETICAL CONSIDERATIONS

In the tunneling model,¹ the TS arise from the tunneling of atoms or groups of atoms in a double well. The energy difference between the eigenstates is given by $E = \sqrt{\Delta^2 + \Delta_0^2}$ with Δ the asymmetry of the double well. Δ_0 is the tunnel splitting, written as $\Delta_0 = \hbar\Omega \exp(-\lambda)$, where λ describes the overlap of the wave functions. One of the basic assumptions of the tunneling model is that Δ and λ are independent of each other and have a uniform distribution $P(\Delta, \lambda)d\Delta d\lambda = \bar{P}d\Delta d\lambda$, with \bar{P} a constant, the density of states of the TS.

To describe the effect of the TS on the low-temperature ultrasonic properties, two different mechanisms have to be considered. First, there is the resonant absorption of the sound wave by those TS having an energy splitting E corresponding to the phonon energy ($E = \hbar\omega$). Because of the wide distribution of energy splittings, this process occurs at all frequencies. When $\hbar\omega \ll kT$, this process leads to a frequency-independent but temperature-

dependent change in the velocity of sound given by⁵

$$\frac{v(T)-v(T_0)}{v(T_0)} = C \ln \frac{T}{T_0} = \frac{\bar{P}\gamma_l^2}{\rho v_l^2} \ln \frac{T}{T_0} \quad (1)$$

with T_0 an arbitrary reference temperature and γ_l the coupling of the TS with the longitudinal phonons. For our absorption measurements, this process need not be considered, since its contribution in this high-energy experiment is negligible compared to the second mechanism, the relaxation process. This process results from the modulation of the energy splittings Δ by the sound wave. The TS are brought out of thermal equilibrium and relaxation occurs via interaction with the thermal phonons. At low temperatures, the most likely process is the one-phonon process, giving rise to a relaxation rate⁶

$$\tau^{-1} = K_3 \left[\frac{\Delta_0}{E} \right]^2 \left[\frac{E}{2k} \right]^3 \coth \left[\frac{E}{2kT} \right] \\ \text{with } K_3 = \frac{4k^3}{3\rho\pi\hbar^4} \sum \frac{\gamma_i^2}{v_i^5}. \quad (2)$$

K_3 describes the coupling of the TS with the phonons, taking into account all polarizations and directions. The general expressions for α and $\Delta v/v$ due to this process are given in Ref. 7 and can be calculated numerically. Analytic solutions, which can be derived for the limiting cases $\omega\tau_m \gg 1$ (with τ_m the smallest relaxation time of the TS) and $\omega\tau_m \ll 1$, are briefly discussed here.

At the lowest temperatures, where the condition $\omega\tau_m \gg 1$ holds, the contribution to the velocity change can be neglected, whereas the relaxational attenuation is expected to be frequency independent and proportional to T^3 .⁷

$$\alpha = \frac{\pi^4}{96} C \frac{K_3}{v_l} T^3 = \frac{\pi^4}{96} \frac{\bar{P}\gamma_l^2}{\rho v_l^3} K_3 T^3. \quad (3)$$

The $\omega\tau_m \ll 1$ condition is satisfied at higher temperatures and leads to a temperature-independent attenuation that varies linearly with frequency.⁷

$$\alpha = \frac{\pi\omega}{2v_l} C = \frac{\pi\omega\bar{P}\gamma_l^2}{2\rho v_l^3}. \quad (4)$$

The variation in the velocity of sound depends logarithmically on temperature in this regime and is frequency independent.⁷

$$\frac{\Delta v}{v} = -\frac{3}{2} C \ln \frac{T}{T_0} = -\frac{3}{2} \frac{\bar{P}\gamma_l^2}{\rho v_l^2} \ln \frac{T}{T_0}. \quad (5)$$

The expressions given so far are valid provided that the TS relax via absorption or emission of a single thermal phonon. At higher temperatures, above a few kelvin, a two-phonon Raman process has to be taken into account.⁷ A modified relaxation time has to be introduced, $\tau^{-1} = \tau_d^{-1} + \tau_r^{-1}$, in which τ_d is the relaxation time for the one-phonon processes [see (2)] and τ_r the relaxation time for the Raman processes. This additional process causes a stronger temperature dependence in the transition re-

gion from the $\omega\tau_m \gg 1$ to the $\omega\tau_m \ll 1$ regime but does not influence the value of the ultrasonic attenuation outside this region.

III. EXPERIMENTAL RESULTS

For our experiments, three synthetic z-cut quartz single crystals, labeled Z-N4, Z-N5, and Z-N6, were irradiated up to doses of 9.9×10^{18} , 3.0×10^{19} , and 4.7×10^{19} n/cm^2 , respectively. These samples are the equivalents of the previously studied x-cut samples N4, N5, and N6. To make reliable comparisons with other measurements³ possible, accurate mass density measurements were carried out. We used a hydrostatic method, obtaining values for the density of 2.634 ± 0.003 , 2.614 ± 0.003 , and 2.585 ± 0.003 g/cm^3 for, respectively, Z-N4, Z-N5, and Z-N6. On these specimens, measurements of the variation of the longitudinal sound velocity were performed as a function of temperature, in a ³He cryostat. Using a pulse-interference method developed in our laboratory⁸ accurate measurements which allow observation of relative velocity changes of the order of 10^{-7} were possible. The absorption measurements were carried out with a pulse-echo technique. For converting the electromagnetic signal into an elastic wave, a LiNbO₃ transducer was attached to the sample with a very thin Nonaq grease bond.

Qualitative analysis of the data

Figure 1 shows the velocity change

$$\frac{\Delta v}{v} = \frac{v(T) - v(T_0)}{v(T_0)}$$

as a function of temperature for the three samples. As reference temperature T_0 , the lowest temperature was taken: 0.38 K for Z-N4, 0.335 K for Z-N5, and 0.315 K

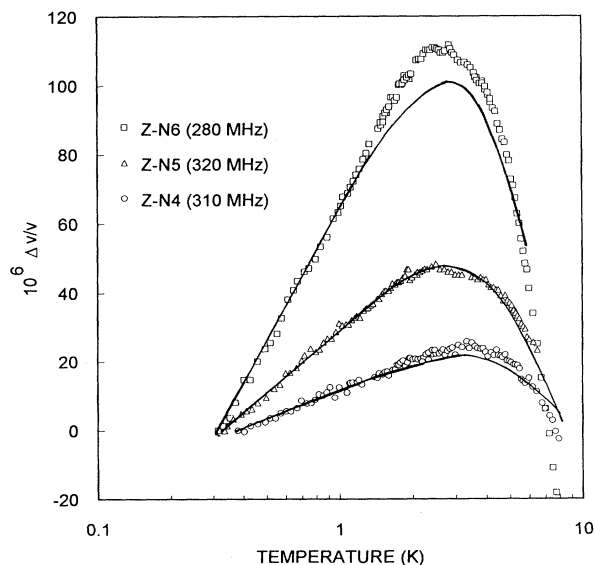


FIG. 1. Ultrasonic velocity change as a function of temperature for Z-N4, Z-N5, and Z-N6; —: fitted curve.

for Z-N6. As can be seen, all three curves show a similar behavior, typical for the presence of TS: at the lowest temperatures (0.3–1.5 K), the velocity increases logarithmically with temperature, as a result of the resonant interaction between the TS and the acoustic phonons [see (1)]. Above 1.5 K, the velocity change deviates from the logarithmic law and a maximum is observed. This behavior is a consequence of the relaxation process, which causes a decrease of the velocity with increasing temperature. When this contribution compensates that of the resonant process, a maximum in $\Delta v/v$ is obtained. At higher temperatures (the $\omega\tau \ll 1$ regime), a logarithmic decrease of the velocity change is expected, with a slope half that of the resonant contribution [see (1) and (5)]. However, as in glasses, a much stronger temperature dependence is found. This has to be attributed to the Raman processes mentioned above, which we will take into account in the quantitative analysis further on.

The absorption⁹ measured for the three doses is shown in Fig. 2. These curves also show the typical TS behavior described by the equations above. At the lowest temperatures, a T^3 dependence is clearly seen, which is typical for the $\omega\tau \gg 1$ regime of the relaxation process [see (3)]. At higher temperatures, the absorption gradually levels off to a temperature-independent plateau, which corresponds to the $\omega\tau \ll 1$ regime [see (4)]. Additional measurements have been carried out to control the frequency dependence of the attenuation.⁹ While the T^3 at the lowest temperatures is found to be frequency independent, the height of the plateau increases linearly with the frequency, in complete agreement with the predictions of the tunneling model.

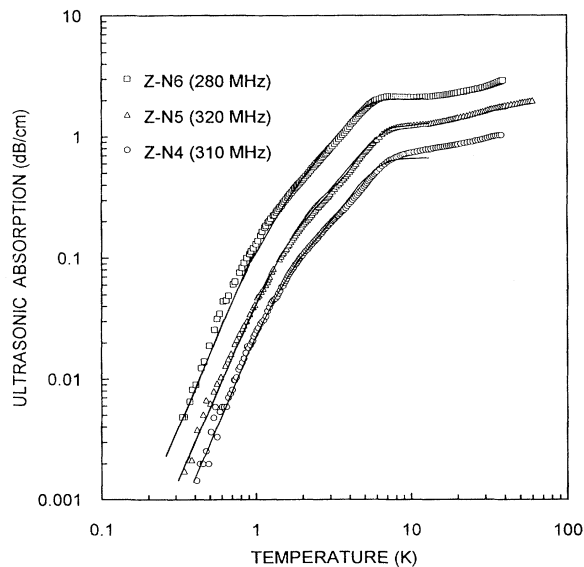


FIG. 2. Ultrasonic absorption as a function of temperature for Z-N4, Z-N5, and Z-N6; —: fitted curve. The subtracted background attenuation α_0 is 0.60 dB/cm for Z-N4, 0.34 dB/cm for Z-N5, and 0.85 dB/cm for Z-N6.

Quantitative study of the measurements

Figures 1 and 2 show the fitted curves obtained from numerical calculations using the tunneling model. From these fits, the TS parameters C and K_3 and the Raman parameter K_7 can be determined independently. As can be seen, the fitted curves are in good agreement with the experimental data. Only the maximum in $\Delta v/v$ for Z-N6 is not very well fitted, but this will not influence our discussion, since only the slope of the logarithmic increase and the position of the maximum determine the parameters derived from the velocity measurements. Table I gives the parameters obtained from the velocity measurements, as well as the value for $\bar{P}\gamma_i^2$, which can be deduced from C . The parameters determined from absorption measurements are given in Table II. Both tables contain also the parameters obtained from previous measurements in x -cut quartz, irradiated with similar doses.^{3,10} We note that there is a discrepancy in the absolute values of the parameters whether derived from absorption or velocity measurements. This inconsistency is, however, not atypical for these measurements, but has been observed for most of the amorphous solids. It is one of the shortcomings of the tunneling model and has been discussed in more detail in a previous paper.³ Other authors as well discuss these discrepancies.^{5,11} This “inconsistency,” however, will not influence the validity of our further discussion, since the latter will be purely based on observed relative changes, and, considering these relative changes, we see that the results of absorption and velocity measurements agree with each other.

A first comparison shows the same tendency for x - and z -cut samples: from velocity and absorption measurements, we can derive that increasing the neutron dose mainly affects C and thus $\bar{P}\gamma_i^2$. For the parameter K_3 , similar values are found in the x - and z -cut samples, as expected since it represents a mean coupling over all directions and polarizations. The slight increase with the dose, which was found before in x -cut quartz,¹² is confirmed in the z -cut samples. This good agreement is an indication for the internal consistency of the measurements and the analysis. A quantitative comparison of the values obtained for $\bar{P}\gamma_i^2$, however, reveals a striking difference: comparing two similar doses, $\bar{P}\gamma_i^2$ is found to be significantly smaller in the z -cut samples than in the x -cut samples. The difference increases with the dose: for Z-N4, $\bar{P}\gamma_i^2$ is approximately 80% of the N4 value, but for Z-N6, only 40% of the N6 parameter is found. Since the irradiations took place in the same reactor, under the same conditions, the damage in the x - and the z -cut samples should be very similar for similar doses, which is in fact confirmed by the mass density measurements. Therefore the density of states of the TS must be the same in samples irradiated with the same dose. This means that $(\bar{P}\gamma_i^2)_z \ll (\bar{P}\gamma_i^2)_x$ can be reduced to a difference in γ_i : the coupling of TS with longitudinal phonons traveling along the crystallographic z axis is markedly smaller than the coupling with phonons in the x direction, pointing out a strongly anisotropic coupling. The difference as observed from our measurements is much too high to be accounted for by the anisotropy of

TABLE I. TS parameters derived from velocity change measurements. The accuracy for C and $\bar{P}\gamma\dot{\gamma}$ is 10%, for K_3 20%. For K_7 only an order of magnitude can be determined.

	Z-N4	Z-N5	Z-N6	N4 [x cut (Ref. 3)]	N5 [x cut (Ref. 10)]	N6 [x cut (Ref. 3)]
Dose (n/cm^2)	310 MHz	320 MHz	280 MHz	648 MHz	648 MHz	195, 400, 648 MHz
Mass density (g/cm^3)	9.9×10^{18}	3.0×10^{19}	4.7×10^{19}	1.2×10^{19}	2.6×10^{19}	4.7×10^{19}
C (10^{-6})	13	28	60	21	49	155
K_3 ($10^7 \text{K}^{-3} \text{s}^{-1}$)	37	40	50	42	42	54^a
$\bar{P}\gamma\dot{\gamma}$ ($10^6 \text{g cm}^{-1} \text{s}^{-2}$)	14	29	62	18	42	130
K_7 ($\text{K}^{-7} \text{s}^{-1}$)	3×10^4	9×10^4	1×10^5	3×10^3	2×10^4	2×10^4

^aCould only be derived from measurements at 195 MHz

TABLE II. TS parameters derived from absorption measurements. The accuracy for C and $\bar{P}\gamma\dot{\gamma}$ is 10%, for K_3 20%. For K_7 only an order of magnitude can be determined.

	Z-N4	Z-N5	Z-N6	N4 [x cut (Ref. 3)]	N5 [x cut (Ref. 10)]	N6 [x cut (Ref. 3)]
Dose (n/cm^2)	310 MHz	320 MHz	280 MHz	648 MHz	648 MHz	195, 400, 648 MHz
Mass density (g/cm^3)	9.9×10^{18}	3.0×10^{19}	$4.7 \text{ties} 10^{19}$	1.2×10^{19}	2.6×10^{19}	4.7×10^{19}
C (10^{-6})	32	58	108	42	97	350 ^a
K_3 ($10^7 \text{K}^{-3} \text{s}^{-1}$)	11	12	18	12	12	15
$\bar{P}\gamma\dot{\gamma}$ ($10^6 \text{g cm}^{-1} \text{s}^{-2}$)	33	60	112	37	84	300 ^a
K_7 ($\text{K}^{-7} \text{s}^{-1}$)	5×10^2	4×10^2	2×10^4	2×10^2	1×10^2	4×10^2

^aCould only be derived from measurements at 195 MHz.

the crystal (the crystalline anisotropy, reflected by the anisotropy in velocity and lattice parameter, is more like 10%, while the anisotropy observed in our data is 200–300%) and must therefore be attributed to the tunneling mechanism itself.

A sceptical reader might ask whether the observed difference between the x -cut and z -cut samples cannot be due to the fact that the measurements are taken at different frequencies. The factor of 2 in our frequencies, however, cannot account for the observed differences between x - and z -cut samples, since a frequency dependence is only observable when the frequencies differ by several orders of magnitude, as is, e.g., the case when the parameters derived from measurements in the kilohertz range are compared with those obtained from experiments in the megahertz range.¹³ Measurements carried out in a frequency range from 100 to 700 MHz do not reveal significant differences in the derived parameters with frequency. One can also wonder whether the fits do not allow one to determine independent values for γ_l and for \bar{P} . γ_l might indeed be calculated from K_3 , which describes the mean coupling between the TS and the phonons by a summation over all directions and polarizations. But to calculate γ_l properly, two “problems” need to be solved. First, one needs to know the value of the transverse coupling γ_t . To solve this problem (γ_t is not known from our experiments), we can assume that $\gamma_t^2/v_t^2 = \gamma_l^2/v_l^2$, as observed in glasses.⁵ A second difficulty arises from the summation over the different directions. For glasses this is not a problem, since they are isotropic, but—as our measurements show—this is not the case in neutron-irradiated quartz: γ_l behaves anisotropically and the velocities v_l and v_t are not exactly known for each direction in the damaged environment. Since a separate, absolute value for γ_l is not essential to the discussion, we therefore preferred not to give one.

IV. DISCUSSION: IMPLICATIONS FOR THE MICROSCOPIC ORIGIN OF THE TUNNELING STATES

As we already mentioned, it was suggested before that the “crystalline” TS (those which are in the crystalline part of the sample) could be located at the microtwins induced in quartz by neutron irradiation.³ The disorder caused by the fast neutrons is twofold: highly disordered clusters are formed which are nearly amorphous and in the crystalline part microtwinning (of the Dauphiné type) is induced, leading to a hexagonal symmetry at doses similar to that of N6.⁴ The breaking of bonds is not required for the formation of the twins. They are formed by small atomic displacements, which cause the passage of small groups of SiO₄ tetrahedra from their original α configuration to the opposite one. These groups have the shape of small chains of tetrahedra in the directions [100] and [110].⁴ According to Grasse, Peisl, and Dorner¹⁴ the same displacements, which are dynamic in an unirradiated crystal near the α - β phase transition, are statically induced by distortions due to the neutron irradiation. The phase transition has been studied extensively in quartz and it is known that the small movements involved take place mainly in the plane perpendicular to the crystallo-

graphic z axis.^{15,16} If such configuration changes are involved in the interaction with the ultrasonic phonons, it can be expected that a longitudinal wave traveling in the plane perpendicular to the z axis can more easily induce a transition of a tetrahedron (or a chain of tetrahedra) than a wave in any other direction, leading to a higher coupling. We can relate this to observations of Duquesne and Belessa.¹⁷ They connect the TS with the rigidity of the network and find that highly constrained “rigid” materials inhibit tunneling motions, while tunneling of structural entities is easily effected in a less constrained “soft” environment. Since movements of tetrahedra are taking place perpendicular on the z axis, we can consider this xy plane as “soft” and thus enhancing the tunneling motions. The z axis is a more “rigid” direction and makes tunneling more difficult. This agrees with what is observed in our experiments: the coupling is higher in the x direction than in the z direction. It is direct experimental evidence for the twins as microscopic origin for at least part of the TS: the chains of tetrahedra which have passed from the α_1 to the α_2 configurations are expected to be able to flip rather easily from one configuration to the other and so form a system with two possible equilibrium positions, a tunneling state. The number of tetrahedra taking part in this process is not known and probably varies, so that different energies are involved, leading to a broad energy distribution, as expected for the TS.

In order to get a better insight into the movements involved in this tunneling, we will now consider in some more detail what happens at the phase transition. The configuration changes there are a consequence of small coupled rotations of adjacent tetrahedra which slightly tilt along the binary axis.^{15,18} The Si atoms remain mainly fixed. In quartz there are chains of tetrahedra along three directions enclosing angles of 120°. Within a row, the coupling between the rotations of the tetrahedra is such as to cause all O ions of the same chain to move in the same sense horizontally, in the plane perpendicular to the z axis.¹⁸ The tilt angle decreases with temperature and is equal to 7° at 570°C, close to the transition,¹⁵ corresponding to a distance between the two possible oxygen sites of about 0.3 Å. This is in agreement with Dolino *et al.*¹⁶ who give a distance of 0.4 Å. From this we can deduce that the TS can be seen as a cooperative tilt of SiO₄ tetrahedra in a chain which involves movements of the oxygen atoms up to about 0.4 Å.

Tables I and II also show that for both absorption and velocity measurements the anisotropy increases with neutron dose. This can be seen as an indication that—in this dose range—the relative contribution of the “crystalline” TS compared to the “amorphous” TS (those in the amorphous regions) increases with increasing dose. The highly anisotropic behavior of N6 agrees with the structural model of this sample. From mass density measurements, the amorphous fraction of N6 is estimated to be about 33%.³ In this sample, the remaining “crystalline” part is thus still twice as large as the amorphous part. Moreover, it is expected to consist fully of twins, since Comes, Lambert, and Guinier⁴ explain the hexagonal structure, observed in a sample irradiated with a similar dose, as a “saturation” of coexisting α_1 - α_2 twin domains. The con-

tribution from this "crystalline" part to the TS will thus be much bigger than the "amorphous" contribution, leading to a highly anisotropic coupling.

Previously it was shown that the TS seen in experiments in neutron-irradiated quartz are similar to those observed in amorphous SiO₂: a similar coupling was found, interpreted as similar TS,¹⁹ and was confirmed by our later experiments in neutron-irradiated quartz, where the coupling was always found to be similar to that in vitreous silica. Both materials are built up by the same basic unit: the SiO₄ tetrahedron. Therefore this paper presents direct experimental evidence for the microscopic origin of the TS in vitreous silica: small rotations or tilts of coupled SiO₄ tetrahedra through distances of about 0.4 Å. This description meets particularly well the predictions based on the studies of structural relaxation and low-frequency harmonic excitations in glasses: Buchenau *et al.*^{20,21} found from their neutron-scattering experiments that these excess excitations in vitreous silica can both be described by coupled rotations of SiO₄ tetrahedra. Their extrapolation²⁰ that the tunneling states in vitreous silica can also be described by such a model now finds experimental evidence: our results provide the missing link for a common interpretation of all three groups of low-frequency excitations found in vitreous silica.

V. SUMMARY

In this work, a study of the TS in neutron-irradiated z-cut quartz has been performed: measurements of the ul-

trasonic attenuation and velocity change have been carried out as a function of temperature. All data can be successfully described by the tunneling model and from numerical fits using this model the typical TS parameters $P\gamma_l^2$ and K_3 are derived. These results are compared to the outcome of a previous study of similar x-cut samples. Qualitatively, the x-cut and z-cut samples show the same tendency: both attenuation and velocity change are found to increase with increasing dose. But a quantitative comparison of the values obtained for $P\gamma_l^2$ reveals a striking difference: comparing two similar doses, the coupling of the TS with the longitudinal phonons turns out to be much smaller in z-cut samples compared to the x-cut specimens. The difference as observed from our measurements is much too high to be accounted for by the anisotropy of the crystal and is therefore attributed to the tunneling mechanism itself. This gives direct experimental evidence for a microscopic picture of the TS in neutron-irradiated quartz in terms of the α_1 - α_2 twins, leading to a description of the tunneling mechanism as small rotations of coupled tetrahedra.

ACKNOWLEDGMENTS

The authors thank H. Grimm for helpful discussions, and G. Groeninckx, D. Dompas, and M. Pirsoul for providing the equipment for mass density measurements. They are also grateful to the SCK (Mol, Belgium) for the neutron irradiation and the IIKW (Belgium) for financial support.

-
- ¹P. W. Anderson, B. I. Halperin, and C. M. Varma, *Philos. Mag.* **25**, 1 (1972); W. A. Phillips, *J. Low Temp. Phys.* **7**, 351 (1972).
²C. Laermans, *Phys. Rev. Lett.* **42**, 250 (1979).
³A. Vanelstraete and C. Laermans, *Phys. Rev. B* **42**, 5842 (1990).
⁴R. Comes, M. Lambert, and A. Guinier, in *Interaction of Radiation with Solids*, edited by A. Bishay (Plenum, New York, 1967), p. 319.
⁵S. Hunklinger and W. Arnold, in *Physical Acoustics*, edited by P. Mason and R. N. Thurston (Academic, New York, 1976), Vol. 2, p. 155.
⁶*Amorphous Solids: Low Temperature Properties*, edited by W. A. Phillips (Springer-Verlag, Berlin, 1981).
⁷P. Doussineau *et al.*, *J. Phys. (Paris)* **41**, 1193 (1980).
⁸A. Vanelstraete and C. Laermans, *Mater. Sci. Eng. A* **122**, 77 (1989).
⁹Preliminary results for one dose are reported in C. Laermans, V. Keppens, and M. Coeck, in *Phonon Physics*, edited by M. Meissner and R. O. Pohl (Springer-Verlag, Berlin, 1993), p.

899.
¹⁰V. Keppens and C. Laermans, *Nucl. Instrum. Methods Phys. Res. Sect. B* **65**, 223 (1992).
¹¹T. L. Smith, P. J. Anthony, and A. C. Anderson, *Phys. Rev. B* **17**, 4997 (1978).
¹²C. Laermans and V. Esteves, *Phys. Lett. A* **126**, 341 (1988).
¹³A. K. Raychaudhuri and S. Hunklinger, *Z. Phys. B* **57**, 113 (1984).
¹⁴D. Grasse, J. Peisl, and B. Dorner, *Nucl. Instrum. Methods Phys. Res. Sect. B* **1**, 183 (1984).
¹⁵H. Grimm and B. Dorner, *J. Phys. Chem. Solids* **36**, 407 (1975).
¹⁶G. Dolino *et al.*, *Bull. Mineral.* **106**, 267 (1983).
¹⁷J. Y. Duquesne and G. Belessa, *Philos. Mag.* **52**, 821 (1985).
¹⁸G. Van Tendeloo, J. Van Landuyt, and S. Amelinckx, *Phys. Status Solidi A* **33**, 723 (1976).
¹⁹B. Golding *et al.*, *Bull. Am. Phys. Soc.* **24**, 495 (1979).
²⁰U. Buchenau *et al.*, *Phys. Rev. Lett.* **60**, 1318 (1988).
²¹U. Buchenau *et al.*, *Phys. Rev. B* **34**, 5665 (1986).